Polymer Degradation and Stability 190 (2021) 109651

Contents lists available at ScienceDirect

Polymer Degradation and Stability

journal homepage: www.elsevier.com/locate/polymdegradstab

A novel aminothiazole-based cyclotriphosphazene derivate towards epoxy resins for high flame retardancy and smoke suppression

Kai Ning[b,1], Lin-Lin Zhou[a,1], Bin Zhao[a,*]

[a] Institute of Functional Textiles and Advanced Materials, Engineering Research Center for Advanced Fire-Safety Materials D & A (Shandong), College of Textiles and Clothing, Qingdao University, 308 Ningxia Road, Qingdao 266071, China
[b] School of Materials Science and Engineering, North University of China, Taiyuan 030051, China

ARTICLE INFO

Article history:
Received 18 April 2021
Revised 29 May 2021
Accepted 6 June 2021
Available online 11 June 2021

Keywords:
Flame retardancy
Epoxy resin
Cyclotriphosphazene
Smoke suppression

ABSTRACT

There is a need to develop halogen-free flame retardants for epoxy resin (EP) to reduce the fire risks. Cyclotriphosphazene-based derivatives have been proved to be effective phosphorous-containing flame retardants. This article demonstrates the preparation and application of a novel aminothiazole-based cyclotriphosphazene derivate (hexathiazoleaminocyclotriphosphazene, HTACP) for EP. After characterizing by Fourier transform infrared spectroscopy (FTIR), nuclear magnetic resonance, and high-resolution mass spectroscopy, HTACP is utilized as a reactive flame retardant for EP. HTACP effectively inhibits the decomposition of EP and improves the char yield during heating according to the thermogravimetric analysis (TGA) results. HTACP also changes the dynamic thermomechanical behaviors of EP according to dynamic mechanical analysis (DMA). With the incorporation of 5 wt% HTACP, EP passes UL-94 V-0 rating during the vertical flame testing and obtains an increased limiting oxygen index of 28.5% with only 0.73% phosphorous content. The cone calorimeter testing results show that HTACP endows EP with beyond 50% reduction of peak heat release rate and total smoke production. The results of smoke density chamber tests also prove the excellent smoke-suppression effects for EP. Furthermore, scanning electron micrograph, X-ray photoelectron spectroscopy, TG-FTIR, and pyrolysis gas chromatography/mass spectrometry are used to analyze the chars and pyrolysis behaviors of EP/HTACP. The phosphazene structure in HTACP molecule is left in the condensed phase, which promotes forming protective chars, while the multiple nitrogen- and sulfur-containing volatiles derives from aminothiazole groups act dilution effects in the flame zone. This novel aminothiazole-based cyclotriphosphazene shows a high efficiency for reducing fire hazards of EP through a bi-phase mechanism.

1. Introduction

Epoxy resins (EPs) are widely used as adhesives, coatings, electronic printed circuit boards, laminates, and composites because of their outstanding adhesion, good chemical resistance, satisfactory dielectric properties, and excellent mechanical properties [1,2]. Unfortunately, untreated EPs are highly flammable and show inevitable strong release of heat and smoke during burning, which are a severe obstacle and potential hazard for the applications [3,4]. Although halogenated (brominated in particular) compounds show high flame retardant efficiency, the chemical risks of halogen-containing flame retardants have caused alarm and discussions [5,6]. Various effective nonhalogen functionalities have been explored, such as additive and reactive flame retardants [7,8], biobased systems [9,10], flame retardant curing agents and monomers [11–13], and nanomaterials [14,15]

Phosphorous-containing flame retardants have become a prominent halogen-free candidate and draw much attention due to their relative low toxicity, multiple action modes, and high efficiency [16,17]. Thereinto, hexachlorocyclotriphosphazene is an important initial molecular for designing flame retardants for EP because of its high P and N contents and chemical versatility. Different side groups such as phenoxyl [18], amino [19,20], alkenyl [21], epoxide [22], and multiple substitutions [3,23] can be chosen to prepare small and cyclocrosslinked cyclotriphosphazene molecules for EP. Furthermore, owing to the high radical quenching efficiency in the gaseous phase, 9,10-dihydro-9-oxa-10-phosphaphenanthrene-10-oxide (DOPO) is also a popular molecular for being integrated on cyclotriphosphazene to obtain excellent bi-phase flame retardant action [24–26]. Recently, nitrogen heterocycle compounds such as imidazole [11,27], thiazole [8,28–30], and triazole [31,32]

* Corresponding author.
E-mail address: binzhao@qdu.edu.cn (B. Zhao).
[1] These authors contributed equally to this work.

https://doi.org/10.1016/j.polymdegradstab.2021.109651
0141-3910/

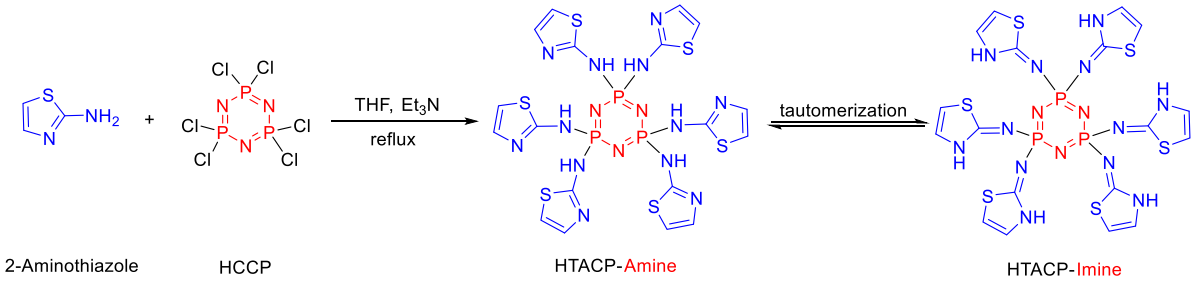

Scheme 1. Synthetic rote and chemical structures of HTACP.

Table 1
Formulas of the EP thermosets.

Samples	DGEBA (g)	DDS (g)	HTACP (g)	HTACP (wt%)	P content (wt%)[a]
EP	40	12.80	0	0	0
EP-1	40	12.80	1.63	3	0.44
EP-2	40	12.80	2.78	5	0.73
EP-3	40	12.80	3.97	7	1.02

[a] Calculated P content in EP thermosets according to P content in HTACP molecular identified by ICP-OES (14.54 wt%).

have been used to design phosphonates and DOPO-based flame retardants for EP, which show high flame retardancy, and reactive behavior. For cyclotriphosphazene-based flame retardants, Cheng et al. successfully prepared an aminobenzothiazole-substituted cyclotriphosphazene derivative, which can be a good reactive flame retardant for EP [33]. There is a need for further designing novel thiazole cyclotriphosphazene derivatives and investigating relevant flame retardant mechanisms.

In the present work, to obtain thiazole-based cyclotriphosphazenes with higher phosphorus content to reduce the fire hazard of EP, a thiazole with simple chemical structure (2-aminothiazole) was used to synthesize a novel cyclotriphosphazene derivative named hexathiazoleaminocyclotriphosphazene (HTACP). HTACP presents high flame retardant efficiency and smoke suppression for EP because of its high phosphorous content and good char forming ability. The thermal stability, dynamic thermomechanical behaviors, pyrolysis behaviors, and flame retardant mechanism of EP/HTACP were comprehensively discussed. This work provides a way to synthesize novel cyclotriphosphazene derivatives with nitrogen heterocycle structure, which have been proved to be effective compounds for reducing the fire hazards of EP.

2. Experimental section

2.1. Materials and reagents

Hexachlorocyclotriphosphazene (HCCP) was commercially provided by Shandong Zeshi New Materials Technology Co., Ltd. 2-aminothiazole and 4,4′-diaminodiphenyl sulfone (DDS) were purchased from Shanghai Xianding Biological Technology Co., Ltd. Triethylamine (TEA) and Tetrahydrofuran (THF) was obtained from Shanghai Aladdin Biochemical Technology Co., Ltd. NPEL128 type of Diglycidyl ether of bisphenol-A (DGEBA) (epoxide equivalent weights: 185 g/equiv) was provided by NanYa Electronic Materials Co., Ltd.

2.2. Synthesis of hexathiazoleaminocyclotriphosphazene (HTACP)

A mixture of 2-aminothiazole (30.0 g, 0.3 mol), triethylamine (35.42 g, 0.35 mol), and tetrahydrofuran (THF, 400 mL) was added into a 1000 mL three-neck bottom flask equipped with a mechanical stirrer, reflux condenser, and thermometer, and then HCCP (17.38 g, 0.05 mol, dissolved in 100 mL THF) was slowly added dropwise at room temperature with stirring. The mixture was heated to reflux temperature for 12 h. After filtrating the mixture, the crude product was washed three times with deionized water and ethanol, then vacuum-dried at 50°C for 24 h to give a brownish yellow solid product (yield, 76%). The corresponding synthetic route of HTACP is illustrated in Scheme 1. ^{1}H-NMR (DMSO-d_6, TMS): δ/ppm 7.23-7.18 (d, 6H), 6.88-6.83 (d, 6H), 7.08 and 7.41 (s, 6H); ^{31}P-NMR (DMSO-d_6, 85% H_3PO_4): δ/ppm -9.76 (s, 1P) and 1.84 (s, 1P); ATR-IR: ν/cm^{-1} = 3115 (—NH—), 1317 (C—N), 1131 and 843 (N-P=N), 977 (P—N—C); ESI-MS ($CH_3C{\equiv}N$, positive mode): *m/z* 729.9508 $[M+H]^+$ (calcd. for $C_{18}H_{18}N_{15}P_3S_6$ 728.9407); ICP-OES: P content 14.54 wt% (calcd.12.73 wt%), Cl content 0 %.

2.3. Preparation of EP and EP/HTACP

To evenly disperse HTACP in DGEBA, a solvent dispersion method was used. Firstly, HTACP and DGEBA were dispersed in an appropriate amount of ethanol with stirring and ultrasonic. After obtaining a homogeneous system, DDS was added and mechanically stirred at 120°C for 20 min. Then, the newly prepared epoxy solution was degassed by evacuation for 5 min. Afterward, the as-obtained epoxy solutions were rapidly poured into a special preheated mold and gradually cured as follows: 160°C for 1 h, 180°C for 2 h, and 200°C for 1 h. The neat EP thermoset was prepared according to the same procedure. Table 1 summarizes all formulas of EP thermosets. Briefly, EP containing 3 wt%, 5 wt%, and 7 wt% HTACP are labeled as EP-1, EP-2, and EP-3, respectively. The curing behaviors of EP and EP-1 were tested by DSC. As shown in Fig. S1 (Supporting information), 3 wt% of HTACP decreased the curing peak of EP from 225 to 217°C, suggesting the reactivity of HTACP in EP.

2.4. Characterization

Attenuated total reflection (ATR) mold of Fourier transform infrared (FTIR) spectra were directly recorded using a Nicolet iS50 spectrometer (Thermofisher). ^{1}H and ^{31}P NMR spectra were tested by a Bruker Avance-IHD spectrometer (600 MHz) using DMSO-d_6 and tetramethylsilane (TMS) as the solvent and internal standard, respectively. Liquid chromatograph-mass spectrometer (LC-MS) analysis was performed using a 1290 UHPLC and Q-TOF 6550 HRMS (Agilent). Inductively coupled plasma optical emission spectra (ICP-OES) measurement was carried on an iCAP 7400 device

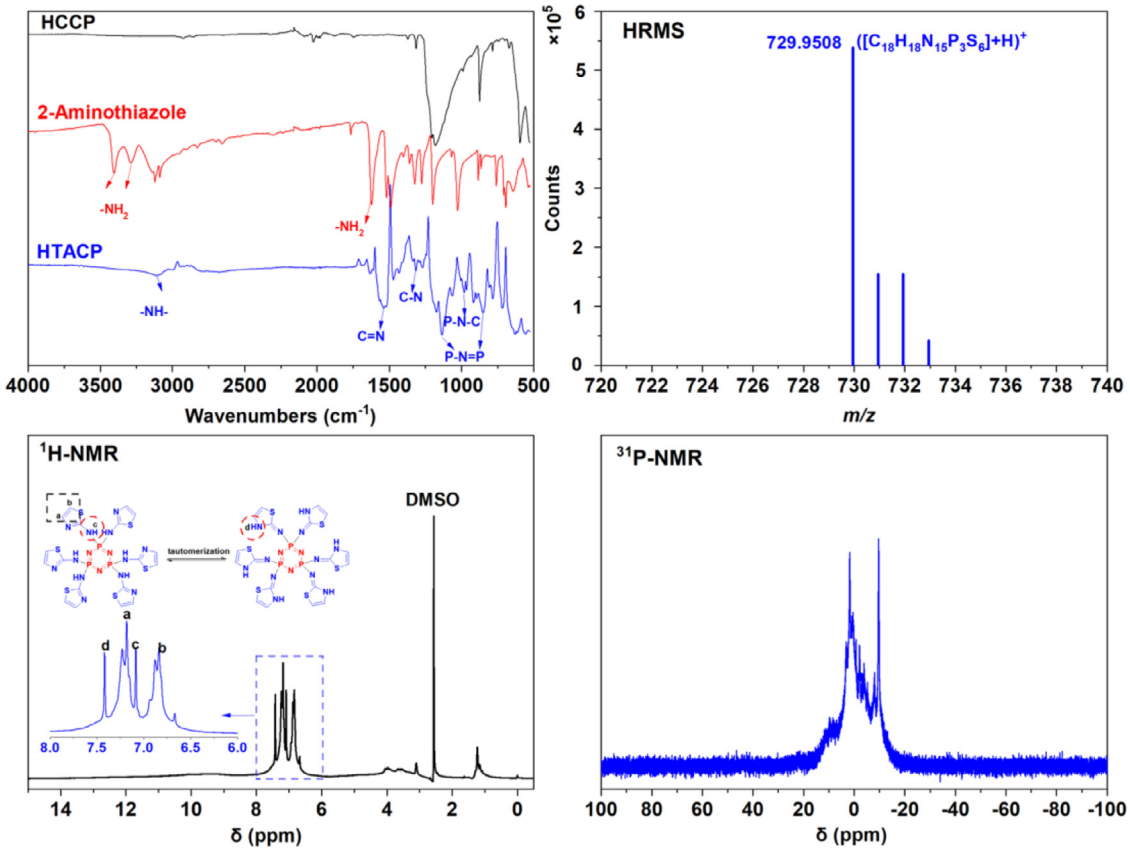

Fig. 1. FTIR, HRMS, ^{1}H-NMR, and ^{31}P-NMR spectra of HTACP.

to determine P and Cl contents of HTACP. Before testing, the sample needs to experience the digestion process by concentrated sulphuric acid.

According to GB/T2406.2-2009, limiting oxygen index (LOI) testing was conducted on a JF-5 oxygen index test instrument (Beijing Airtimes, China). Vertical flame testing was performed on a CZF-5 instrument (Nanjing Jiangning Instrument Factory, China) following the ASTM D3801/UL-94V standard. The dimensions of samples for LOI and UL-94 were 130 × 6.5 × 3.2 mm^3 and 125 × 13 × 3.2 mm^3, respectively. Cone calorimeter testing (FTT, East Grinstead, UK) was used to evaluate the fire behaviors of EP specimens with a dimension of 100 × 100 × 3 mm^3 following ISO 5660-1, and the heat flux of radiant cone was set as 35 kW m^{-2}.

The micromorphologies of EP char layers were observed using a scanning electron microscopy instrument (Vega 3TESCAN, Czech) at 5 kV. X-ray photoelectron spectroscopy (XPS) analysis was carried out on an ESCALAB 250Xi photoelectron spectrometer (Thermo Fisher Scientific, USA), using monochromatic Al Kα X-ray souse ($h\nu$=1486.8 eV).

The non-isothermal curing behavior of EP mixtures was investigated by differential scanning calorimetry (DSC, Mettler-Toledo DSC 1). Each relevant EP mixture (DGEBA/DDS with/without HTACP, 5±0.5 mg) was put into an alumina crucible and heated from 50-275°C at 10°C min^{-1} under nitrogen atmosphere.

Thermogravimetric analysis (TGA) was conducted on a STA 6000 instrument (Perkin-Elmer, USA) from 40-700°C at a heating rate of 10°C min^{-1} in N_2. All the samples were controlled to 5±0.5 mg. HTACP powder was directly tested, and the EP samples were scraped from relevant thermosets with a scraper blade. Furthermore, A Perkin-Elmer Frontier FTIR spectrometer connected to STA 6000 (TG-FTIR) was utilized to distinguish the pyrolysis volatiles of typical samples. Both the gas cell and transferline in TG-FTIR were maintained at 280°C to prevent condensation of the released volatiles. The samples were prepared to fine powder of 10±0.5 mg. Each sample was heated from 40 to 700°C in nitrogen at a 20°C min^{-1} ramp.

HTACP (~2 mg) was first pyrolyzed in a CDS 5200 pyrolyzer at 500°C under a helium atmosphere. Then, the volatiles were loaded through He to a gas chromatography-mass spectrometer (PerkinElmer Clarus 680 GC-SQ8MS). In detail, the temperature of the capillary column (HP-5, 0.25 mm) of the GC was controlled to 40°C for 3 min before being increased to 280°C at 10°C min^{-1} rate (keep 280°C for 5 min). The temperature of GC/MS interface and the injector was maintained at 280°C.

A Perkin-Elmer DMA 8000 thermomechanical analyzer was used to test the thermomechanical properties of EP samples at a frequency of 1 Hz using a three-point bending mold from 50 to 280°C by 5°C min^{-1}. The specimen's size was 40 × 10 × 4 mm^3.

Smoke density chamber tests were conducted using an FTT0064 device with a pilot flame at 25 kW m^{-2} based on ISO5659-2:2006. The samples used for testing had dimensions of 75×75× 3 mm^3.

3. Results and discussions

3.1. Characterization of HTACP

The chemical structure of HTACP was characterized through FTIR, ^{1}H-NMR, ^{31}P-NMR, and HRMS (Fig. 1). For HTACP, peaks at 843 and 1134 cm^{-1} can be ascribed to the asymmetrical N—P=N stretching (phosphazene rings), and the C—N absorption peak can be found at 1317 cm^{-1}. Notably, the N—H (primary amine) stretching vibration shoulder peaks at 3289 and 3404 cm^{-1} of 2-aminothiazole entirely disappeared on the spectrogram of HTACP, while the new peaks at 3115 and 977 cm^{-1} are assigned to the

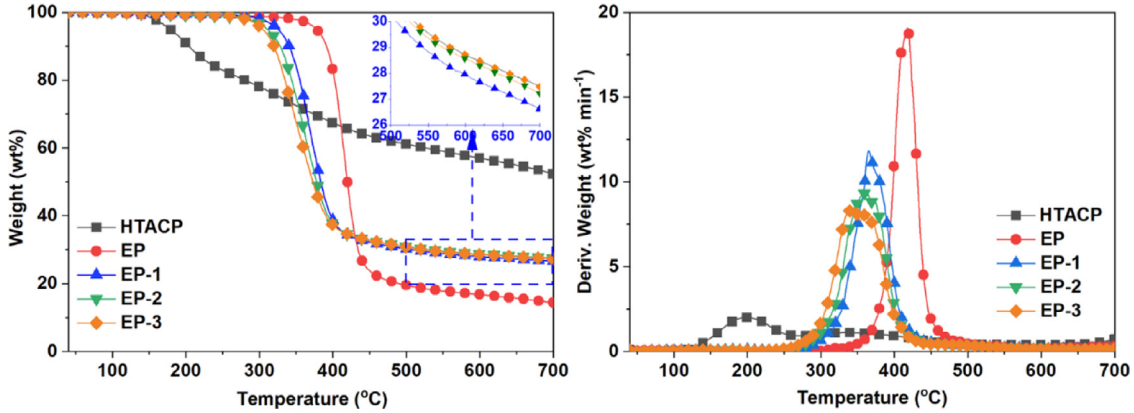

Fig. 2. TG (left) and DTG (right) curves of HTACP, EP, and EPs containing HTACP under nitrogen atmosphere.

Table 2
Typical parameters obtained from TG analyses under nitrogen atmosphere.

Samples	$T_{-5\%}$ (°C)	T_{max} (°C)	Mass loss rate at T_{max} (wt% min^{-1})	Residue at 700 °C (wt%)	
				Expt values	Calcd values [a]
HTACP	179	200	2.0	52.3	-
EP	378	418	19.1	14.4	-
EP-1	326	365	11.8	26.6	15.5
EP-2	311	361	9.4	27.5	16.2
EP-3	305	345	8.5	27.2	17.0

[a] Calcd values=$m_{(\text{expt residue of EP})}\ w_{(EP)} + m_{(\text{expt residue of HTACP})}\ w_{(HTACP)}$.

stretching vibration of imine group (—NH—) and P—N—C outside the cyclotriphosphazene ring, respectively. The ^{1}H-NMR spectrum of HTACP displays double peaks belonged to methine proton in thiazole ring signals at δ=7.30-7.12 and δ=6.94-6.72 (H-a and H-b), respectively. Two single peaks at 7.08 and 7.42 ppm are belonged to N—H in the tautomer of HTACP-Amine and HTACP-Imine, respectively. The special tautomerization of thiazole-based phosphorus-containing compounds have been previous reported, which is related to the electron accepting substituents bonded with the exocyclic nitrogen atom of thiazole [34,35]. As shown in ^{31}P-NMR, owing to the tautomerization of HTACP, there are two typical peaks at chemical shifts of -9.70 and 1.76 ppm corresponding to different phosphorus environments of HTACP-Amine and HTACP-Imine, respectively, which is in accordance with ^{1}H-NMR and FTIR analyses. Also, the HRMS spectrum (ESI, positive mode) of HTACP indicates the equimolecular ion peak $[M+H]^+$ at *m/z* 729.9508 (calcd. for $C_{18}H_{18}N_{15}P_3S_6$ 728.9407). Besides, the result of ICP-OES shows that there is 14.54 wt% phosphorus (close to the calcd. value of 12.7 wt%) and no chlorine in HTACP. Based on the analyses above, HTACP has been successfully synthesized.

3.2. Thermal analysis

The thermal stabilities of HTACP, EP, and flame retardant EPs were evaluated using thermogravimetric analysis under a nitrogen atmosphere, as shown in Fig. 2 and Table 2. HTACP starts to decompose at 179°C considered as a lower initial decomposition temperature ($T_{-5\%}$), whereas presents good char forming ability for leaving higher char residue of 52.3 wt% at 700°C. EP shows typical one-stage decomposition TG and DTG curves, the $T_{-5\%}$ and temperature at maximum decomposition rate (T_{max}) on which are 378 and 418°C, respectively. Owing to the lower decomposition temperature of HTACP, flame retardant EPs exhibit strongly reduced thermal stability and gradually decreased $T_{-5\%}$ and T_{max} values with increasing loadings of additives. As shown in Table S1, HTACP shows lower thermal stability (lower $T_{-5\%}$ value), but the $T_{-5\%}$ reduction ($\Delta T_{-5\%}$) of EP/HTACP is closed or even lower than that of some previous reported EP/thiazoles-based compounds thermosets [30,32,33]. This can be explained that HTACP is considered as a reactive flame retardant for epoxy resin due to the secondary amines in the molecular. After co-curing with EP by the stepwise curing process from 160 to 200°C mentioned in the experimental section, HTACP can be thermal stable in the cross-linked macromolecular network of epoxy resin. HTACP effectively inhibits the maximum decomposition rate of EP, and finally promotes EP producing greater char at high temperatures (400-700°C). From Table 2, besides, the experimental values of residue for EP/HTACP are higher than the corresponding calcd ones, suggesting that HTACP or its decomposition products can react with epoxy resin matrix to improve the char yield.

DMA is utilized to further investigate the dynamic thermomechanical behaviors of EP-HTACP thermosets. Fig. 3 presents the storage modulus (E') and tan delta versus temperature curves. The relevant data are summarized in Table 3. T_g denotes the glass-transition temperature, which is the corresponding temperature for the maximum value of tan δ. The crosslinking densities (ν_e) of EPs have been calculated according to the equation derived from the rubber elasticity theory [32,36]. A small amount of reactive flame retardant can act as chemical crosslinking points in the network of epoxy resin. Then, the incorporation of 3 wt% HTACP enhances the E' value of EP due to the increased crosslinking density, which can be attributed to the reactivity of HTACP. With the increase of HTACP loadings, however, both decline of ν_e and E' values of EP results from the consumption of epoxy groups and the retarded crosslinking reaction by the reactivity and steric hindrance effect of extra HTACP molecule [33]. The T_g values of EPs gradually proportionally lower with the improvement amounts of HTACP due to the comprehensive influences of the competitive factors.

3.3. Flame retardancy and fire behavior

Vertical flame testing (VFT, UL-94) and limiting oxygen index (LOI) are important tests for assessing the flame retardancy of polymers. Table 4 provides a summary of flame retardancy data

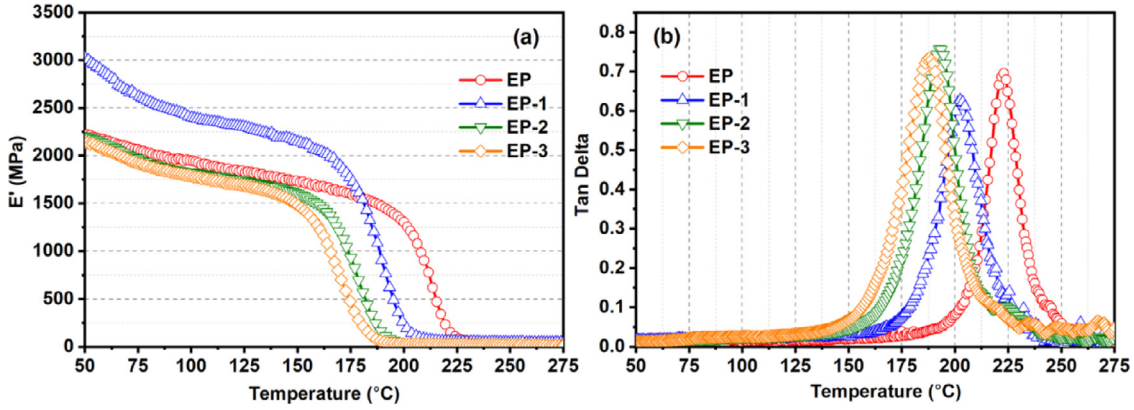

Fig. 3. The storage modulus (E') and tan δ versus temperature curves of EPs.

Table 3
Thermomechanical properties of EPs.

	T_g (°C) [a]	E′ at 50°C (MPa)	E′ at (T_g + 30 K) (MPa)	v_e (mol m^{-3}) [b]
EP	223	2222	45.8	3491
EP-1	202	3025	49.4	3922
EP-2	192	2200	27.0	2187
EP-3	187	2137	22.8	1866

[a] T_g denotes the glass-transition temperature.
[b] v_e denotes the crosslinking density; v_e=E'/3RT, E' means the storage modulus taken 30 K beyond T_g, R is the gas constant (8.314 J mol^{-1} K^{-1}), T is the temperature of (T_g+30 K).

Table 4
Flame retardancy of EPs according to LOI and VFT.

Samples	P content (wt%) [a]	LOI (%)	UL-94 (3.2 mm)			
			t_1 (s)	t_2 (s)	Rating	Dripping
EP	0	22.5	≥90	-	No rating	No
EP-1	0.44	27.5	16±1	2±0.5	V-1	No
EP-2	0.73	28.5	8±0.5	0	V-0	No
EP-3	1.02	28.8	5±1	0	V-0	No

[a] Calculated P content in EP thermosets according to P content in HTACP molecular identified by ICP-OES (14.54 wt%).

of EP samples. EP presents a lower LOI value of 22.5% and burns to clamp (without fire dripping but the fire chars dropped) during 90 s after being ignited during vertical flame testing. The flame retardancy of EP is gradually enhanced with the increase of HTACP loadings. With only 3 wt% dosages of HTACP, EP-1 obtains an increased LOI value of 27.5% and passes UL-94 V-1 rating. When 5 wt% HTACP is added, EP-2 achieves a higher LOI value of 28.5%, and passes a UL-94 V-0 rating with the quick self-extinguishing behavior during VTF. By importing 7 wt% HTACP, EP-3 self-extinguishes in 5 s and passes UL-94 V-0 rating. Nevertheless, the LOI value of EP-3 slightly increased to 28.8%. Similar results have been previously reported owing to the decreased cross-linking density of EP thermoset by introducing reactive flame retardants [12,32,33]. Finally, with only 0.73 and 1.02 wt% phosphorus contents, EP-2 and EP-3 passes UL-94 V-0 rating and good fire-resistance performance (self-extinguishing in 1 s after the second ignition) during VFT, indicating high flame retardant efficiency of HTACP for EP.

The combustion behavior of EPs was evaluated by cone calorimeter testing, Fig. 4 and Table 5 present the typical curves and corresponding results, respectively. The strongly reduced time to ignition (t_{ig}) values of flame retardant EPs can be ascribed to their lowered thermal stability, in accordance with the TGA results. The early decomposed flammable volatiles released into gaseous phase makes the EP/HTACP samples easily been ignited. Compared to EP, the peak heat release rate (pHRR) values of EP-1, EP-2, and EP-3 decline by 55.0%, 56.5%, and 60.8%, respectively. Total heat release (THR) values of EP are also significantly decreased by introducing HTACP. The dramatically decreased pHRR and THR values indicate that HTACP shows high inhibition efficiency for heat release of EP. In addition, fire growth rate (FIGRA), defined as the maximum of HRR(t)/t, is important for evaluating the fire-spreading behavior. As listed in Table 5, EP-1, EP-2, and EP-3 show lower FIGRA values than that of EP, suggesting that the delayed fire time to flashover of EP and much more escape time for evacuating people in a fire. For smoke behavior, it is noted that total smoke production (TSP) values of flame retardant EPs decrease by 50% in comparison with those of EP, suggesting high efficiency of smoke suppression for HTACP in EP. Meanwhile, the slightly decreased average CO yield (av-COY) values of EP-2 and EP-3 indicate that the introducing of HTACP can reduce the smoke toxicity of EP to some extent. Visibly, the char residues of EP/HTACP thermosets significantly increased in comparison with that of EP, suggesting that HTACP facilities epoxy matrix generate more stable char during combustion.

To further asses the smoke releases behaviors of EP with HTACP, EP and EP-3 were selected for the smoke density chamber tests according to ISO5659-2. As shown in Fig. S2, the specific optical density (Ds) of EP reaches to maximum Ds at 286 s with a very high value of 1018.5 and tends to be relatively stable. After introducing HTACP, it is noted that the maximum Ds of EP-3 is as low as 637.1,

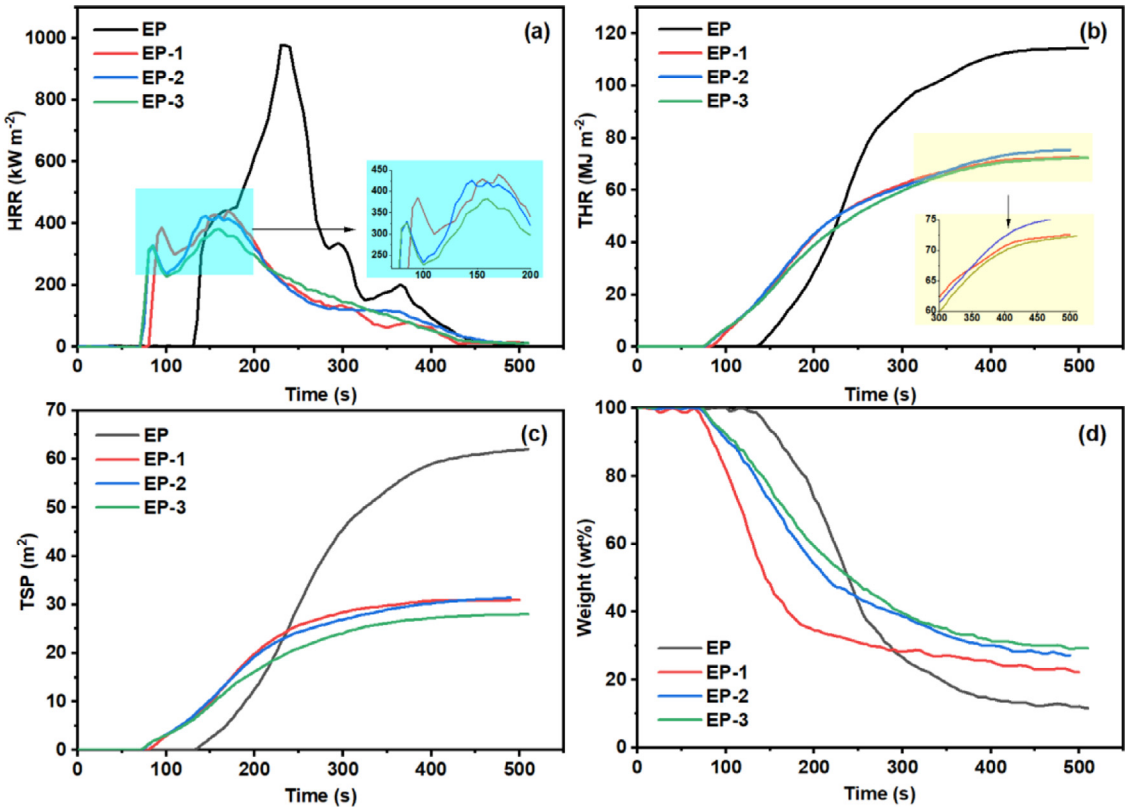

Fig. 4. Heat release rate (HRR) (a), total heat release (THR) (b), total smoke production (TSP) (d), and residue (d) plots of EPs obtained from cone calorimeter tests.

Table 5
Cone calorimeter data of EP, EP-1, EP-2, and EP-3.

Samples	t_{ig}(s)	t_p(s)	pHRR(kW m^{-2})	FIGRA(kW m^{-2} s^{-1})	THR(MJ m^{-2})	TSP(m^2)	Av-COY[a](kg kg^{-1})	Residue (wt%)
EP	129	230	977	4.3	114	62	0.071	12
EP-1	78	170	440	4.1	73	31	0.081	22
EP-2	70	145	425	3.8	75	31	0.068	27
EP-3	69	160	383	3.9	72	28	0.067	28

a: Average values between time to ignition (t_{ig}) and time to flame out (t_f).

which declines to 62.5% of that for EP. This result suggests that the incorporation of HTACP effectively decrease the smoke release of EP during burning. Combining with the TSP results from cone calorimeter tests, HTACP exhibits excellent smoke suppression effects for EP.

3.4. Char residue analyses

SEM was adopted to observe the micromorphologies of the char residues of EPs collected after cone calorimeter testing. Fig. 5 illustrates the digital pictures of char residues, the corresponding interior and exterior SEM images. Although EP leaves char residue after combustion due to the bisphenol A and crosslinking structure, as shown in Fig. 5(a1–a3), the char presents a rimose interior surface and loose exterior surface which is failed to hinder the heat and oxygen transfer. Compared to EP, EP-HTACP thermosets form more intumescent char layers during combustion (Fig. 5b3, c3, d3). Furthermore, the more smooth (interior surface) and compact (exterior surface) char layers can be obtained with the gradually increase loadings of HTACP in EP. The visible changes of char morphologies indicate that HATCP effectively promotes EP forming protective char layers to restrain the heat and smoke release, which following the cone calorimeter results.

The chemical constitution of the char residues was further characterized by XPS. The survey spectra for the char residues of EP and EP-3 in Fig. 6(a) shows four lines are assigned to C_{1s}, O_{1s}, N_{1s}, and P_{2p} (only in EP-3 residue) symbols, and the high-resolution spectra of corresponding photoelectron peaks are presented in Fig. 6(b–e), respectively. As shown in C_{1s} spectra, both EP and EP-3 show typical graphite signal at 284.8 eV (C—C). The peaks related to C—O, and C—N groups appear at 285.7 and 286.3 eV for EP and EP-3, respectively. Small signals near 290 eV for both EP and EP-3 can be assigned to C=O and C=C due to the crosslinked structures result from aromatization. Compared to the EP residue, an additional peak at 531.8 eV arises in the O_{1s} spectrum of EP-3 residue due to the presence of P—O [37]. The typical two peaks around 400 eV are ascribed to C—N and N—H bonds, as shown in the N1s spectrum of EP residue. Regarding the EP-3 residue, a new peak arises at 398.8 eV due to the nitrogen atoms in the phosphazene ring [38]. Typically, the two peaks around 134 eV in the spectrum of EP-3 residue are attributed to the phosphorus atoms in the phosphazene structure [39]. As analyzed above, it is concluded that HTACP promotes EP forming phosphazene-containing firm char layers, resulting in better flame retardant action in the condensed phase.

3.5. Gaseous products analysis

Fig. 7(A) and (B) illustrate 3D diagrams and typical FTIR spectra of the volatiles of HTACP and EPs during TGA tests, respectively.

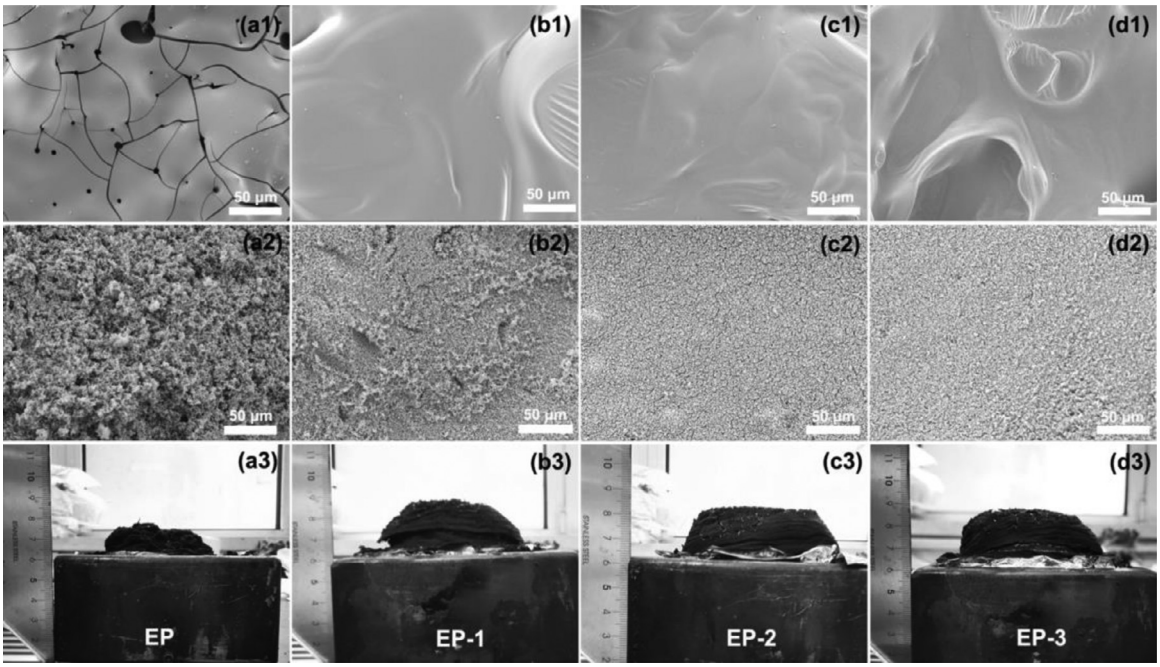

Fig. 5. SEM images of interior chars (a1–d1) and exterior chars (a2–d2); digital photos of EPs after cone calorimeter tests (a3–d3)

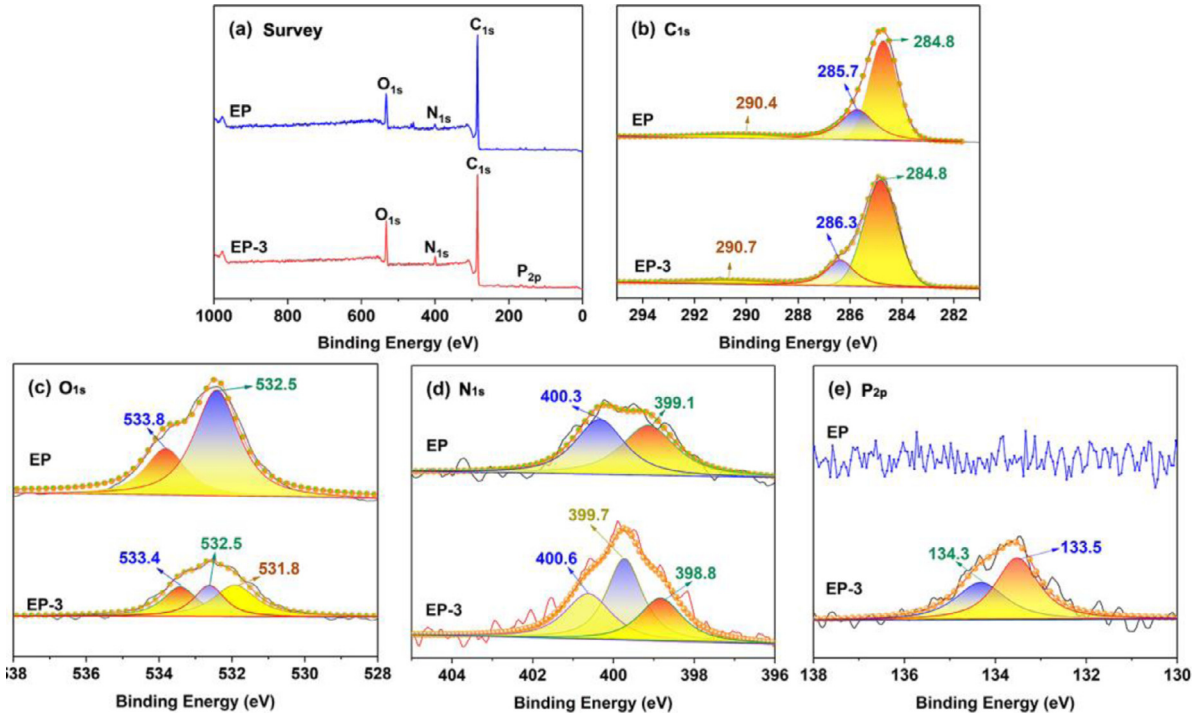

Fig. 6. Survey and high-resolution XPS spectra of C_{1s}, O_{1s}, N_{1s}, and P_{2p} of the char residues for EP and EP-3 after vertical flame testing.

As shown, peaks of $-CH_2-$ (2966 cm^{-1}), C=N, C=C, and/or C=S (1506 cm^{-1}), NH_3 (962, 754 cm^{-1}) [29,40], and a tiny peak of C≡N and/or C≡C (2065 cm^{-1}) are gradually detected on the spectra of HTACP during heating, which can be derived from aminothiazole structure. There is no typical phosphorus-containing substance release into the gaseous phase, suggesting the phosphazene structure in HTACP molecular exists in char residue. This result is in accordance with the XPS analyses above. The characteristic absorbance peaks of hydroxyl (3659 cm^{-1}), hydrocarbon (2966 cm^{-1}), carbonyl (1752 cm^{-1}), ester (1260 cm^{-1}), ether (1171 cm^{-1}), and aromatic compound (1603, 1499 cm^{-1}) are found in the pyrolysis spectrum of EP [18]. Compared to EP, there is no obvious different absorbance peak in the IR pyrolysis spectrum of EP-3. The main reason for this result is that the C=C, C=N, and/or C=S (the predominant peak in HTACP spectrum) show coincidence peak position with that of aromatic compound. To further understand the intensity changes of volatiles, the total, hydrocarbons, and aromatic compounds are selected for evaluation, as shown in Fig. 7(C). After incorporating HTACP, the maximum thermal decomposition time of EP is lowered from 20 min to 18 min. The different decomposition time is ascribed to the lower thermal stability of HTACP and early decomposition of EP-3 presented in the TGA results (Fig. 2).

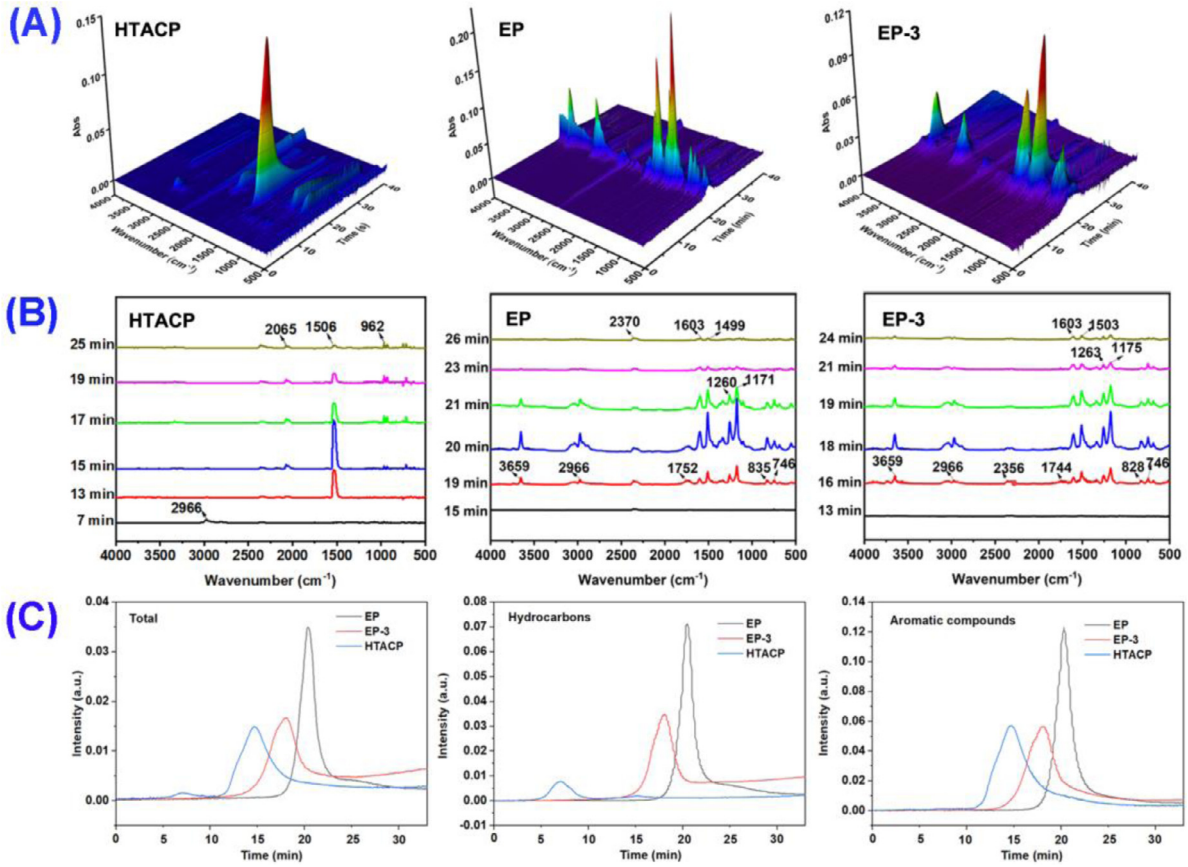

Fig. 7. 3D diagrams (A), FTIR spectra (B), and intensity of the characteristic peaks of gaseous volatiles (C) for HTACP, EP, and EP-3 during heating.

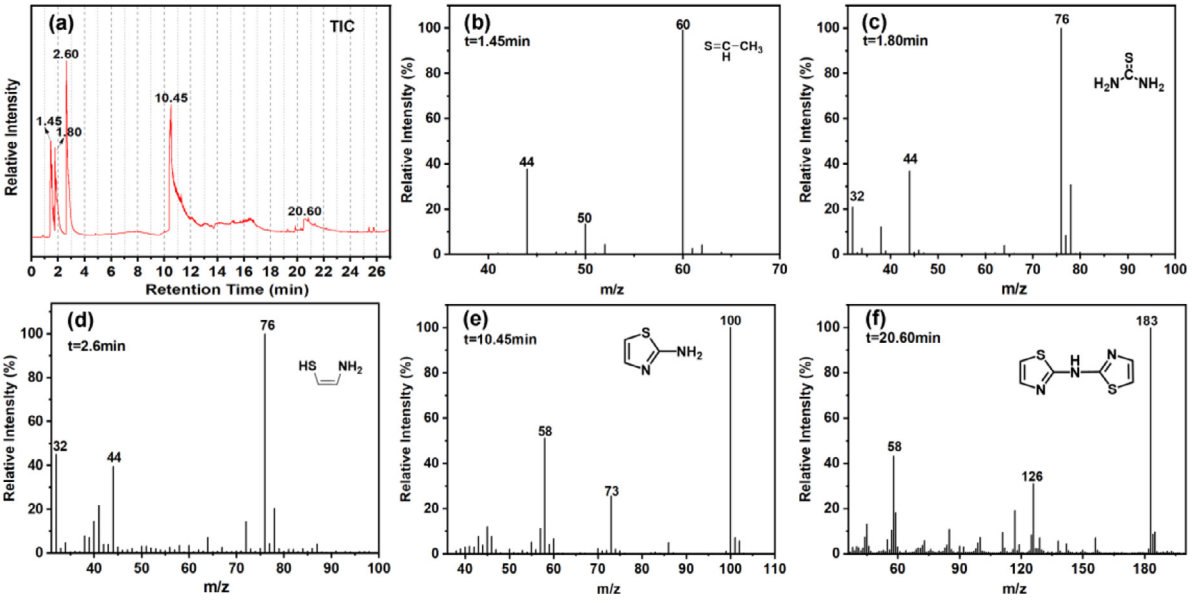

Fig. 8. Total ion chromatogram (TIC) of HTACP (a), and the relevant GC/MS spectra at different retention time (b–f).

According to the Beer-Lambert law, the concentrations of hydrocarbons and aromatic compounds (typical flammable volatiles) of EP-3 are significantly reduced in the gaseous phase due to the lowered absorbance intensities. Then, as a speculation, the diminished release of the flammable gases results in lower "fuel" to feedback into the flame zone [41].

To further analyze the pyrolysis behavior of HTACP, a Py-GC/MS testing was adopted using the pyrolysis temperature at 500°C. As shown in Fig. 8(a), the total ion chromatogram (TIC) at 1.45 min, 2.80 min, 10.45 min, and 20.60 min, the related MS spectra are summarized in Fig. 8(b–f). By comparing the corresponding MS spectra against the NIST library, five pyrolysis products are identified to ethanethial ($[M]^+$=60, Fig. 8b), thiourea ($[M]^+$=76, Fig. 8c), 2-amino-1-ethanethiol ($[M+H]^+$=76), 2-aminothiazole ($[M]^+$=100), 2- thiazolamine ($[M]^+$=183), respectively. These sulfur- /nitrogen-containing volatiles derive from

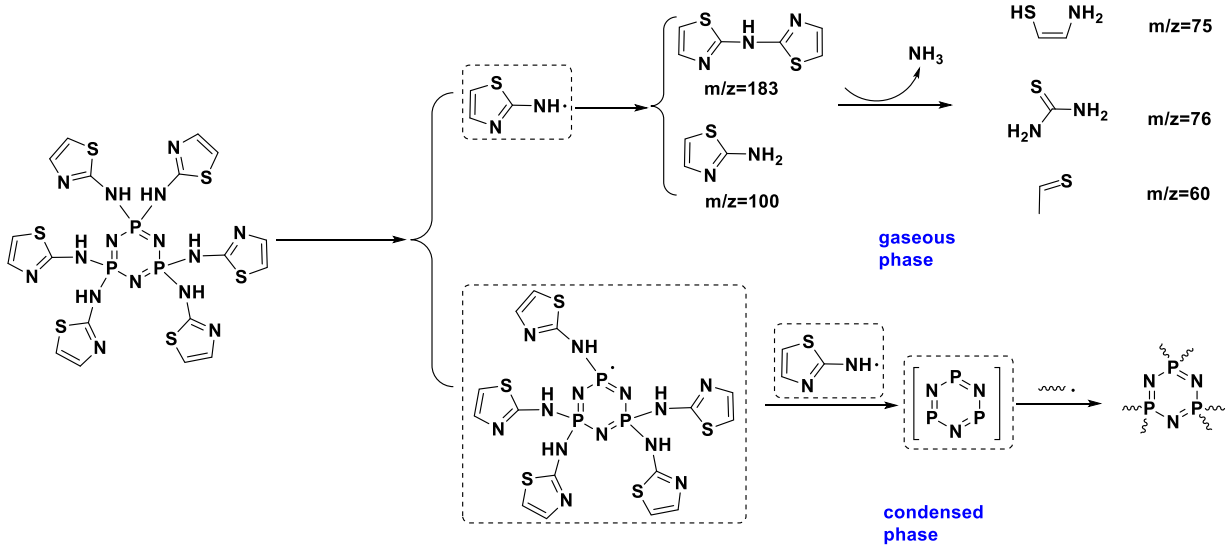

Scheme 2. Proposed pyrolysis process of HTACP

aminothiazole moiety in HTACP molecular, which can further decompose to C=C, C=S, C=N, $-CH_2-$ containing substance and NH_3. Besides, no phosphorus-containing compounds signal is detected, which is in accordance with TG-IR and XPS analyses.

According to the pyrolysis results, together with the XPS and TG-IR analyses, a proposed pyrolysis process of HTACP is illustrated in Scheme 2. During pyrolysis, homolytic cleavage occurs on the P—N bond of HTACP to produce aminothiazole radical, which further evolves to the sulfur- /nitrogen-containing volatiles in the gaseous phase. After introducing HATCP into EP, these multiple nitrogen- and sulfur-containing incombustible gases can effectively dilute oxygen in the flame zone [29]. The phosphazene-containing radical and substance can further react with oxygen-, carbon-, and/or other pyrolysis products from epoxy resin to form thermal stable phosphorus-rich chars in the condensed phase. Thus, HTACP can act as a good flame retardant for EP based on both gaseous and condensed phase mechanisms.

4. Conclusions

A novel flame retardant named hexathiazoleaminocyclotriphosphazene (HTACP) was successfully synthesized, characterized, and used to reduce the fire safety of EP. Thermal analysis revealed that HTACP effectively inhibited the decomposition of EP and enhanced the char yield. The changed loadings of HTACP showed different influences for dynamic thermomechanical behaviors of EP. Only 5 wt% HTACP (0.73% phosphorus content) endowed EP with UL-94 V-0 rating during the vertical flame testing. Furthermore, the HTACP dramatically reduced the heat and smoke release of EP according to cone calorimeter analysis and smoke density chamber tests. The char and gaseous product analyses disclosed that the phosphazene structure promoted protective chars forming in the condensed phase, while the multiple N- and S-containing volatiles derived from the aminothiazole structure showed dilution effects in the flame zone. HTACP can be used for reducing fire hazards of EP through a bi-phase flame retardant mechanism.

Declaration of Competing Interest

The authors declare that they have no known competing financial interests or personal relationships that could have appeared to influence the work reported in this paper.

CRediT authorship contribution statement

Kai Ning: Investigation, Data curtion, Writing – original draft. **Lin-Lin Zhou:** Investigation, Data curtion. **Bin Zhao:** Conceptualization, Writing – review & editing, Supervision, Funding acquisition.

Acknowledgement

The authors would like to acknowledge the financial support from the National Natural Science Foundation of China (Grant No. 21975226). The authors would also like to acknowledge Jie-Hao He for smoke density chamber tests assistance at Sichuan University.

Supplementary materials

Supplementary material associated with this article can be found, in the online version, at doi:10.1016/j.polymdegradstab.2021.109651.

References

[1] F.L. Jin, X. Li, S.J. Park, Synthesis and application of epoxy resins: a review, J. Ind. Eng. Chem. 29 (2015) 1–11.
[2] R. Auvergne, S. Caillol, G. David, B. Boutevin, J.P. Pascault, Biobased thermosetting epoxy: present and future, Chem. Rev. 114 (2) (2014) 1082–1115.
[3] G. Yang, W.H. Wu, Y.H. Wang, Y.H. Jiao, L.Y. Lu, H.Q. Qu, X.Y. Qin, Synthesis of a novel phosphazene-based flame retardant with active amine groups and its application in reducing the fire hazard of epoxy resin, J. Hazard. Mater. 366 (2019) 78–87.
[4] E.D. Weil, S. Levchik, A review of current flame retardant systems for epoxy resins, J. fire. Sci. 22 (1) (2004) 25–40.
[5] J.D. Boer, H.M. Stapleton, Toward fire safety without chemical risk, Science 364 (6437) (2019) 231.
[6] T.G. Osimitz, S. Kacew, A.W. Hayes, Assess flame retardants with care, Science 365 (6457) (2019) 992.
[7] Z.B. Shao, M.X. Zhang, Y. Li, Y. Han, L. Ren, C. Deng, A novel multi-functional polymeric curing agent: synthesis, characterization, and its epoxy resin with simultaneous excellent flame retardance and transparency, Chem. Eng. J. 345 (2018) 471–482.
[8] R.K. Jian, Y.F. Ai, L. Xia, Z.P. Zhang, D.Y. Wang, Organophosphorus heteroaromatic compound towards mechanically reinforced and low-flammability epoxy resin, Compos. B Eng. 168 (2019) 458–466.
[9] S. Wang, S. Ma, C. Xu, Y. Liu, J. Dai, Z. Wang, X. Liu, J. Chen, X. Shen, J. Wei, Vanillin-derived high-performance flame retardant epoxy resins: facile synthesis and properties, Macromolecules 50 (2017) 1892–1901.
[10] X. Wang, W. Guo, L. Song, Y. Hu, Intrinsically flame retardant bio-based epoxy thermosets: a review, Compos. B Eng. 179 (2019) 107487.
[11] Y.J. Xu, J. Wang, Y. Tan, M. Qi, L. Chen, Y.Z. Wang, A novel and feasible approach for one-pack flame-retardant epoxy resin with long pot life and fast curing, Chem. Eng. J. 337 (2018) 30–39.

[12] Y. Tian, Q. Wang, L. Shen, Z. Cui, L. Kou, J. Cheng, J.Y. Zhang, A renewable resveratrol-based epoxy resin with high Tg, excellent mechanical properties and low flammability, Chem. Eng. J. 383 (2020) 123124.
[13] Y. Qiu, L. Qian, H. Feng, S. Jin, J. Hao, Toughening effect and flame-retardant behaviors of phosphaphenanthrene/phenylsiloxane bigroup macromolecules in epoxy thermoset, Macromolecules 51 (23) (2018) 9992–10002.
[14] G. Huang, W. Chen, T. Wu, H. Guo, C. Fu, Y. Xue, K. Wang, P. Song, Multifunctional graphene-based nano-additives toward high-performance polymer nanocomposites with enhanced mechanical, thermal, flame retardancy and smoke suppressive properties, Chem. Eng. J. 410 (2021) 127590.
[15] L. Zhang, Q. Wang, R.K. Jian, D.Y. Wang, Bioinspired iron-loaded polydopamine nanospheres as green flame retardants for epoxy resin via free radical scavenging and catalytic charring, J. Mater. Chem. A 8 (5) (2020) 2529–2538.
[16] S. Huo, P. Song, B. Yu, S. Ran, V.S. Chevali, L. Liu, Z. Fang, H. Wang, Phosphorus-containing flame retardant epoxy thermosets: recent advances and future perspectives, Prog. Polym. Sci. 114 (2021) 101366.
[17] M.M. Velencoso, A. Battig, J.C. Markwart, B. Schartel, F.R. Wurm, Molecular firefighting-how modern phosphorus chemistry can help solve the challenge of flame retardancy, Angew. Chem. Internat. Ed. 57 (33) (2018) 10450–10467.
[18] W.J. Liang, B. Zhao, C.Y. Zhang, R.K. Jian, D.Y. Liu, Y.Q. Liu, Enhanced flame retardancy of DGEBA epoxy resin with a novel bisphenol-A bridged cyclotriphosphazene, Polym. Degrad. Stabil. 144 (2017) 292–303.
[19] W.J. Liang, B. Zhao, P.H. Zhao, C.Y. Zhang, Y.Q. Liu, Bisphenol-S bridged penta(anilino)cyclotriphosphazene and its application in epoxy resins: synthesis, thermal degradation, and flame retardancy, Polym. Degrad. Stabil. 135 (2017) 140–151.
[20] B. Zhao, W.J. Liang, J.S. Wang, F. Li, Y.Q. Liu, Synthesis of a novel bridged-cyclotriphosphazene flame retardant and its application in epoxy resin, Polym. Degrad. Stabil. 133 (2016) 162–173.
[21] J. Liu, Z. He, G. Wu, X. Zhang, C. Zhao, C. Lei, Synthesis of a novel nonflammable eugenol-based phosphazene epoxy resin with unique burned intumescent char, Chem. Eng. J. 390 (2020) 124620.
[22] G.R. Xu, M.J. Xu, B. Li, Synthesis and characterization of a novel epoxy resin based on cyclotriphosphazene and its thermal degradation and flammability performance, Polym. Degrad. Stabil. 109 (2014) 240–248.
[23] X. Zhou, S. Qiu, X. Mu, M. Zhou, W. Cai, L. Song, W.Y. Xing, Y. Hu, Polyphosphazenes-based flame retardants: a review, Compos. B Eng. 202 (2020) 108397.
[24] L. Qian, L. Ye, Y. Qiu, S. Qu, Thermal degradation behavior of the compound containing phosphaphenanthrene and phosphazene groups and its flame retardant mechanism on epoxy resin, Polymer 52 (24) (2011) 5486–5493.
[25] L.J. Qian, L.J. Ye, G.Z. Xu, J. Liu, J.Q. Guo, The non-halogen flame retardant epoxy resin based on a novel compound with phosphaphenanthrene and cyclotriphosphazene double functional groups, Polym. Degrad. Stabil. 96 (6) (2011) 1118–1124.
[26] M.J. Xu, G.R. Xu, Y. Leng, B. Li, Synthesis of a novel flame retardant based on cyclotriphosphazene and DOPO groups and its application in epoxy resins, Polym. Degrad. Stabil. 123 (2016) 105–114.
[27] Y.J. Xu, L. Chen, W.H. Rao, M. Qi, D.M. Guo, W. Liao, Y.Z. Wang, Latent curing epoxy system with excellent thermal stability, flame retardance and dielectric property, Chem. Eng. J. 347 (2018) 223–322.
[28] R. Jian, P. Wang, W. Duan, J. Wang, X. Zheng, J. Weng, Synthesis of a novel P/N/S-containing flame retardant and its application in epoxy resin: thermal property, flame retardance, and pyrolysis behavior, Ind. Eng. Chem. Res. 55 (44) (2016) 11520–11527.
[29] R. Jian, P. Wang, L. Xia, X. Yu, X. Zheng, Z. Shao, Low-flammability epoxy resins with improved mechanical properties using a Lewis base based on phosphaphenanthrene and 2-aminothiazole, J. Mater. Sci. 52 (16) (2017) 9907–9921.
[30] R.K. Jian, Y.F. Ai, L. Xia, L.J. Zhao, H.B. Zhao, Single component phosphamide-based intumescent flame retardant with potential reactivity towards low flammability and smoke epoxy resins, J. Hazard. Mater. 371 (2019) 529–539.
[31] P. Wang, Z. Cai, Highly efficient flame-retardant epoxy resin with a novel DOPO-based triazole compound: thermal stability, flame retardancy and mechanism, Polym. Degrad. Stabil. 137 (2017) 138–150.
[32] Y.F. Ai, L. Xia, F.Q. Pang, Y.L. Xu, H.B. Zhao, R.K. Jian, Mechanically strong and flame-retardant epoxy resins with anti-corrosion performance, Compos. B Eng. 193 (2020) 108019.
[33] J. Cheng, J. Wang, S. Yang, Q. Zhang, Y. Hu, G. Ding, S. Huo, Aminobenzothiazole-substituted cyclotriphosphazene derivative as reactive flame retardant for epoxy resin, React. Funct. Polym. 146 (2020) 104412.
[34] K. Gholivand, S. Farshadian, M.F. Erben, C.O.D. Védova, Synthesis and characterization of the first phosphonic diamide containing thiazolyl groups: Structural properties and tautomeric equilibrium, J. Mol. Struct. 978 (1) (2010) 67–73.
[35] R. Jian, P. Wang, W. Duan, L. Xia, X. Zheng, A facile method to flame-retard epoxy resin with maintained mechanical properties through a novel P/N/S-containing flame retardant of tautomerization, Mater. Lett. 204 (2017) 77–80.
[36] P.J. Flory, Molecular theory of rubber elasticity, Polymer 20 (11) (1979) 1317–1320.
[37] W. Zhao, J. Liu, H. Peng, J. Liao, X. Wang, Synthesis of a novel PEPA-substituted polyphosphoramide with high char residues and its performance as an intumescent flame retardant for epoxy resins, Polym. Degrad. Stabil. 118 (2015) 120–129.
[38] R. Milani, M. Gleria, S. Gross, R.D. Jaeger, A. Mazzah, L. Gengembre, M. Frere, C. Jama, Surface functionalization with phosphazenes: part 6. Modification of polyethylene-co-polyvinylalcohol copolymer surface plates with fluorinated alcohols and azobenzene derivatives using chlorinated phosphazenes as coupling agents, J. Inorg. Organomet. Polym. 18 (3) (2008) 344–351.
[39] P. Vassileva, V. Krastev, L. Lakov, O. Peshev, XPS determination of the binding energies of phosphorus and nitrogen in phosphazenes, J. Mater. Sci. 39 (9) (2004) 3201–3202.
[40] A. Marcilla, M.I. Beltran, A. Gómez-Siurana, I. Martinez-Castellanos, D. Berenguer, V. Pastor, A.N. García, TGA/FTIR study of the pyrolysis of diammonium hydrogen phosphate-tobacco mixtures, J. Anal. Appl. Pyrol. 112 (2015) 48–55.
[41] A.N. Zhang, H.B. Zhao, J.B. Cheng, M.E. Li, S.L. Li, M. Cao, Y.Z. Wang, Construction of durable eco-friendly biomass-based flame-retardant coating for cotton fabrics, Chem. Eng. J. 410 (2021) 128361.